

# Assessment of the Level of Radioactivity in the Soil in Urban Areas and Building Materials of Arlit City (Agadez-NIGER)

M. O. Sidibé<sup>1</sup>, A. O. Manga<sup>1</sup>, S. Soumana<sup>2</sup>, O. K. Adukpo<sup>3</sup>

<sup>1</sup>Abdou Moumouni University of Niamey, Climate-Environment and Materials-Radiation Laboratory.

Research team: Materials and Nuclear Physics, BP : 10622 Niamey, Niger

<sup>2</sup>Radioisotope Institute, BP: 10723 Niamey, Niger

<sup>3</sup>Ghana Atomic Energy Commission, Radiation Protection Institute, P. O. Box LG Legon-Accra, Ghana

## ARTICLE INFO

### Article history:

Received 19 September 2023

Received in revised form 7 August 2024

Accepted 7 August 2024

### Keywords:

Natural radioactivity  
Gamma spectrometry  
Radium equivalent activity  
External and internal risk  
Soil and building materials samples

## ABSTRACT

Niger's uranium deposits are located in the north, bordering the southern Sahara. Mining activities led to the creation of the town of Arlit in 1969. Uranium mining and uranate production generate large volumes of radioactive solid and liquid tailings, as well as radioactive gases. Through dispersion and transport, these radioactive discharges become a source of contamination to the environment and food chain. The aim of our work is to assess the additional ambient exposure to radioactivity of surrounding populations as a result of mining activities. We assessed the risk of exposure to radionuclides from the uranium-238 decay chain through soil and certain building materials. The methodology used is based on collection of soil, sand, gravel and mud samples, which are analyzed using gamma spectrometry technique. Nine (9) public sites and five (5) building materials quarries were sampled for the work. The radiological parameters calculated are radium equivalent activity ( $Ra_{eq}$ ), absorbed dose rate (D), internal and external risk indices ( $H_{in}$  and  $H_{ex}$ ) and gamma index ( $I_\gamma$ ). For the whole study area, the calculated  $Ra_{eq}$  values range from 78.67 Bq/kg to 199.32 Bq/kg. These values are below the guideline value of 370 Bq/kg. In terms of air dose rate, however, the average value found was 0.32 mSv/year for the nine public sites considered. This exceeds the threshold value of 0.29 mSv/year corresponding to the selected exposure scenarios. In addition, in the mud (Quarry 5) and the second gravel quarry (Quarry 4),  $I_\gamma$  values greater than unity were found. A comparison is made with the results of similar studies around the world. Interpretation of the data obtained concludes that there is a risk of radiological overexposure at six (6) sites and two (2) quarries. This work is independent research which sheds new light on the issue of uranium mining activities impact on the environment in Arlit.

© 2024 Atom Indonesia. All rights reserved

## INTRODUCTION

The uranium zone in Niger was discovered in the late 1950s by research team from the French Commissariat à l'Énergie Atomique (CEA). It is located in the Agadez region, in the Saharan part of Niger (Fig. 1). Uranium mining led to the creation of the town Arlit, located within the boundary of the mines. Nearly fifty years of mining operations have generated large volumes of radioactive tailings. Through their dispersion, these residues pose a major problem of radiological pollution to the

environment and food chain. This pollution results in additional radioactivity exposure to the surrounding population. Indeed, the population can be exposed through contaminated soils and building materials used for farming and building. When the activity of the radioactive substances contained in the soil or in these materials is known, it is possible to deduce or predict the dose rate emitted using specific conversion factors, assuming that uranium is in equilibrium with its daughter products. It has been observed that 98.5 % of the radiological effects of uranium-238 (U-238) series elements are due to radium-226 (Ra-226) and its progeny [1]. For this reason, the contribution of precursors between U-238 and Ra-226 can be neglected.

\*Corresponding author.

E-mail address: [sidibmahamadou@yahoo.fr](mailto:sidibmahamadou@yahoo.fr)

DOI: <https://doi.org/10.55981/aj.2024.1374>

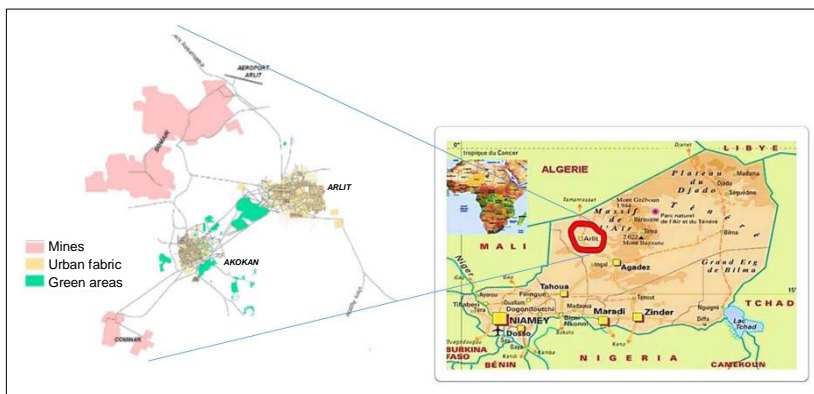


Fig. 1. Location of Arlit on the map of Niger.

The aim of our study is to assess the risk of exposure due to specific radionuclides, such as Ra-226, thorium-232 (Th-232) and potassium-40 (K-40), in soils and building materials through the determination of various indices: equivalent radium activity  $Ra_{eq}$ , absorbed gamma dose rate in air (D), external and internal contamination indices  $H_{ex}$  and  $H_{in}$  and the  $I_{\gamma}$  index, which is used to estimate the risk level of gamma radiation. The concentration of natural radioactivity in the samples considered was determined using the gamma spectrometry technique. Similar studies have been published [2-10]. There are very few independent studies assessing the impact of uranium mining activities in Niger. Our work, thus, makes a major contribution to this field. It is also the first time that the methodology of determining radiological parameters of building materials has been used to assess the level of exposure to radioactivity in the context of the town of Arlit. The results are discussed and compared with those reported in similar studies and with international guideline value [6-10]. In our case, the results of this study provide baseline data on the natural radioactive isotopes present in the building materials used in the region where large uranium deposits exist. The results will serve as reference data for improving radiation protection measures.

## MATERIALS AND METHOD

### Study area

The uranium deposits are located in the northern territory of Niger, in the region of Agadez, which is around 850 km as a straight line from Niamey. Uranium mineralization is contained in the carboniferous series of the Tim Mersoï Basin [11]. The sedimentary cover is subdivided into several sandstone-clay sequences, and the Arlit unit is located on the Namurian Tarat formation [12, 13]. This unit is characterized by the presence of eolian quartz grains. In addition, according to the World Harmonized Soil Database [14], the dominant soil groups for northern Niger are leptosols and arenosols. The soils are composed of 80 % dunes and 20 % of moderate clayey hydromorphic soils [15].

We collected soil, sand, gravel and mud samples, at a depth of 30 cm to take account of variations in the degree of contamination, in order to characterize the levels of radioactivity, whether present naturally or enhanced as a result of mining activities, in nine (9) public sites of interest (schools, land for modern market and bus station construction projects), as shown in Fig. 2, and five (5) quarry sites (see Fig. 3). Each area was sampled at three (3) different points, sufficiently distanced apart to have representative samples of the concerned sites (42 samples).

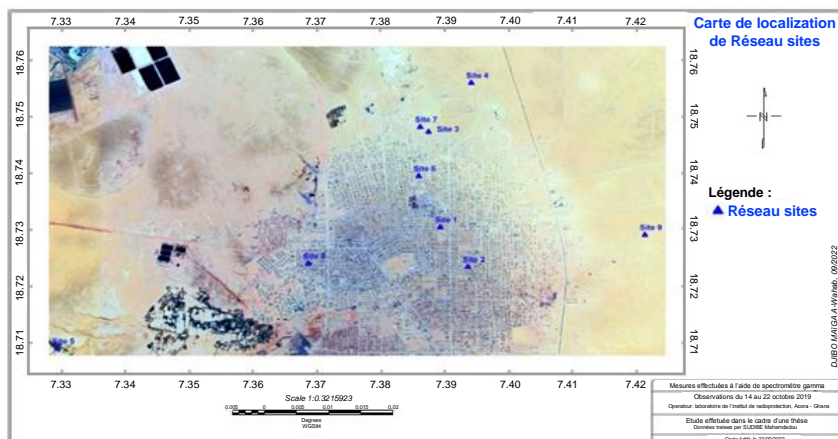
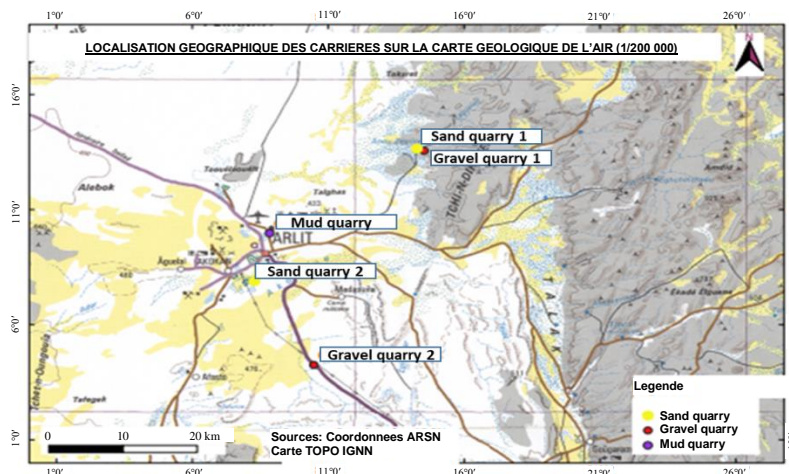


Fig. 2. Location of the 9 public sites.



**Fig. 3.** Geographical location of quarries.

### Sample preparation

The samples taken are first reduced to a considerably fine fraction. Then, they are air-dried at 105 °C for 24 hours, if necessary. After this stage, the samples are placed in 360 ml cylindrical polyethylene capsules to reach secular equilibrium between radon-222 (Rn-222) and its progeny, at the end of 32 days. A radioactive decay chain leaning towards an equilibrium state, called secular equilibrium, characterized by the equality of the activities of all the isotopes in the chain, i.e., a state where, for each intermediate isotope in the chain, the quantity of isotope generated is equal to the quantity of isotope that disappears through decay. This equilibrium state is reached after a time  $t$  equivalent to  $6T$ , where  $T$  represents the longest half-life of the intermediate isotopes. In gamma spectrometry, this is taken into account in sample preparation.

### Gamma spectrometry system

To determine the concentration of natural radioactivity in the samples, a gamma spectrometry system consisting of n-type coaxial High Purity Germanium detector and operated by Genie 2000 software was used. The resolution (FWHM) of this system is 1.96 keV of Co-60 (1332 keV) with a relative efficiency of 42.6 %. The system has been calibrated for a range of geometries using a mixed standard radionuclide source manufactured by Czech Metrology Institute (reference source). The operating range of the detector is set to 40 keV to 3000 keV.

### Sample analysis

#### **Background spectrum acquisition**

The background spectrum is obtained by acquiring a no-load system. Acquisition can be carried out using a container of identical

composition to those used for sample measurement, and an inactive matrix. For our work, we used spectra available in the laboratory and suitable for our study.

#### **Measurement chain calibration**

The detection chain used consists of a coaxial HPGe detector polarized at +2500 volts and housed in a shielded enclosure (the lead castle). The detector is cooled with liquid nitrogen in a 25-liter dewar. To identify the radioelements present in the sample, it is necessary to perform an energy calibration of the measurement chain and an efficiency calibration.

#### **Energy calibration**

An energy window is represented by a channel in which pulses of the same size are stored. Energy calibration of the detection chain therefore consists in translating the correspondence between channels and their energies ( $E = f(N^\circ \text{ channel})$ ). This correspondence will enable to assign the corresponding energy to each peak. We perform this operation using three standard sources (Am-241, Cs-137, and Co-60).

#### **Efficiency calibration**

In practice, it is not possible to calculate efficiency values for different energy ( $\varepsilon = f(E)$ ) and for all the geometries (in terms of sample holders) used in the laboratory. Standard samples are prepared to empirically determine the efficiency of the measurement chain. For our work, we used a ready-to-use filter standard. The multi-gamma source used is europium-152. The spectrum of this source has a number of well-defined peaks in energy and intensity. What is needed is to re-acquire its

spectrum for a counting time  $t = 86400$  seconds. Then, we calculated the efficiency for all energies using Eq. (1) [16, 17].

$$\varepsilon = \frac{N}{N_0} = \frac{N_{\text{net}} - N_{\text{bf}}}{A * I * \Delta t * M} \quad (1)$$

### The energy value of radionuclides of interest

Under the assumption that secular equilibrium was reached between U-238, Th-232, and their respective decay daughter products, the following relatively intense gamma-ray transitions were used to measure the activity concentrations for the aforementioned radionuclides.

U-235 and Ra-226 emit gamma-rays with energies of 185.7 keV ( $I = 57.2\%$ ) and 186.2 keV ( $I = 3.6\%$ ), respectively. It is not easy to separate these peaks. Therefore, the concentration of Ra-226 was calculated as a weighted mean of the activity concentrations of the gamma rays of Pb-214 (295.1 keV, 351.9 keV), Bi-214 (609.3 keV and 1120.29 keV). The gamma-ray photopeaks used for the determination of the Th-232 contents were 338.4 keV, 911.2 keV, and 969.11 keV of Ac-228 and 238.6 keV of Pb-212; K-40 was directly determined (1460.83 keV).

### Acquisition of the spectrum of the sample

The conditioned sample is placed on the detector cover, and the acquisition software is used to set a counting time (86400 s or 24 hours). After counting, the spectrum obtained is loaded, and the radionuclides of interest are identified.

The use of a nuclide library is essential in this process. Knowing, through the radionuclide library, the intensity  $I$  of gamma emission, the energy  $E$  of the identified radionuclide and the mass  $m$  of the sample, then its activity is evaluated by using Eq. (2).

$$A(\text{Bq/kg}) = \frac{N-B}{\varepsilon.I.t.m} \quad (2)$$

where:

$A$  is the specific activity

$N$  is the net area of the peak at the energy  $E$  of the radionuclides with the presence of the samples.

$B$ : The net area of the peak at the energy  $E$  of the radionuclides in the absence of the samples (background).

$\varepsilon$  is the efficiency of the detector evaluated as a function of the transition energy.

$I$  is the intensity of radiation, the number of gammas per disintegration of the nuclide at energy  $E$

$t$  is the counting time of the sample.

$m$  is the mass of the sample.

### Consideration of uncertainties

The radionuclides emitted several gamma energy lines. Individual activity values were derived using Eq. (2) above with associated combined uncertainties given in Eq. (3).

$$\sigma(\text{Ai}) = \sqrt{\left(\frac{\Delta N}{N}\right)^2 + \left(\frac{\Delta I}{I}\right)^2 + \left(\frac{\Delta \varepsilon}{\varepsilon}\right)^2 + \left(\frac{\Delta m}{m}\right)^2} \quad (3)$$

where  $\Delta N$ ,  $\Delta I$ ,  $\Delta \varepsilon$  and  $\Delta m$  are the uncertainties of the count rate, efficiency, gamma-ray emission probability and sample weight, respectively (with assumption that the uncertainty of the counting time can be neglected).

### Calculation of the Minimum Detectable Activity (MDA)

The MDA is the minimum detectable activity (in Bq/kg), It is the activity below which a radionuclide is not detected. It can be calculated for the radionuclides present in the recorded spectrum, but also for all other isotopes not detected, part of the library used. To find an MDA value, two other values are used: the decision threshold (SD) and the detection limit (DL). Below the decision threshold, it is estimated that a signal  $N$  is not significant, and the detection limit corresponds to the value of the smallest signal that can be reliably quantified. The calculation of the SD is done by taking into account the background noise ( $N_b$ ), and in a simplified manner, by using Eq. (4).

$$SD \approx 2\sqrt{2N_b} \quad (4)$$

From the SD, we calculate the DL:  $DL = 2 SD$ . If the signal  $N$  is less than the DL, we then calculate the MDA from the DL, as expressed in Eq. (5).

$$MDA = \frac{DL}{\Delta t.I.\varepsilon.m} \quad (5)$$

### The radium equivalent activity

The distribution of natural radionuclides in the building material samples studied is not uniform. This is why a common radiological index has been introduced to represent the specific radioactivity level of Ra-226, Th-232, and K-40. This common index takes into account the associated radiological risks. This is known as the Beretka formula (see Eq. 6) [6], the activities of Ra-226 (370 Bq/kg), Th-232 (259 Bq/kg) and K-40 (4810 Bq/kg) represent the same effective dose of  $\gamma$  radiation.

$$Ra_{\text{eq}} = A_{Ra} + 1,43A_{Th} + 0,077A_K \quad (6)$$



where  $A_{Ra}$ ,  $A_{Th}$ , and  $A_K$  are the specific activity concentrations of  $^{226}Ra$ ,  $^{232}Th$ , and  $^{40}K$  in Bq/kg respectively.

### Absorbed dose rate in air (D)

The absorbed gamma dose rate in air 1 m above the ground surface for the uniform distribution of radionuclides (Ra-226, Th-232, and K-40) was calculated using Eq. (7) [18].

$$D(nGy.h^{-1}) = 0.462A_{Ra} + 0.604A_{Th} + 0.0417A_K \quad (7)$$

where  $A_{Ra}$ ,  $A_{Th}$ , and  $A_K$  represent the specific activities of Ra-226, Th-232 and K-40, respectively.

The population-weighted values give an absorbed dose rate in air outdoor from terrestrial gamma radiation of 59 nGy/h [18]. The corresponding effective dose is calculated from the absorbed dose by applying the factor 0.7 Sv/Gy [19].

The target group considered in this study is made up of sedentary people from schools, the market, and the bus station as well as the general population, merchants, and transporters. With 8760 hours of presence per year, which counts for outdoor and indoor space occupations (external occupancy factor of 0.8 and internal occupancy factor of 0.2).

### Radiological hazard index

The external contamination index ( $H_{ex}$ ) is determined for all the quarry samples analyzed according to Eq. (8) [6].

$$H_{ex} = \left( \frac{A_{Ra}}{370} + \frac{A_{Th}}{259} + \frac{A_K}{4810} \right) \leq 1 \quad (8)$$

The risk of internal exposure to radon and its descendants is quantified by the ( $H_{in}$ ) index. It is given by Eq. (9) [6].

$$H_{in} = \left( \frac{A_{Ra}}{185} + \frac{A_{Th}}{259} + \frac{A_K}{4810} \right) \leq 1 \quad (9)$$

The values of  $H_{ex}$  and  $H_{in}$  must be less than unity in order to consider the risks to be negligible. Another parameter used is the index ( $I_\gamma$ ) proposed by NEA-OECD [20] and given by Eq. (10). Its value must also be less than unity. It is used to estimate the level of gamma radiation risk associated with naturally occurring radionuclides present in the materials of interest.

$$I_\gamma = \left( \frac{A_{Ra}}{150} + \frac{A_{Th}}{100} + \frac{A_K}{1500} \right) \leq 1 \quad (10)$$

## RESULTS AND DISCUSSION

### The radium equivalent activity

Figures 4 and 5 show the specific activities of the three radionuclides of interest ( $^{226}Ra$ ,  $^{232}Th$ , and  $^{40}K$ ). These values represent the average of the analysis results of the three (3) samples taken per site. The world average concentrations of Th-232, K-40 and Ra-226 are 45, 412 and 32 Bq/kg, respectively, as published by UNSCEAR (2010) [19].

The radium equivalent activity corresponding to the world average of Ra-226, Th-232, and K-40 is 129 Bq/kg. Regarding the sites, the calculated  $Ra_{eq}$  values vary from 78.67 Bq/kg (site 5) to 199.32 Bq/kg (site 9), with an average of 143.10 Bq/kg.  $Ra_{eq}$  of sites 4, 5, and 6 is lower than the world average value, while it is the opposite for sites 1, 2, 3, 7, 8, and 9 (Fig. 4). In the case of the quarries, the minimum value of  $Ra_{eq}$  is obtained for sand (Quarry 1) at 41.57 Bq/kg, while the highest value of  $Ra_{eq}$  is found for gravel (Quarry 4) at 164.54 Bq/kg for an average of 115.25 Bq/kg.  $Ra_{eq}$  of quarries 1 and 2 is lower than the world average value. But for quarries 3,4 and 5, the value exceeds the world average Fig. 5.

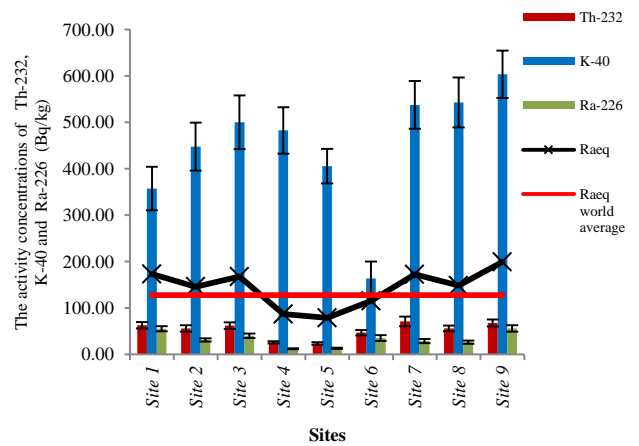


Fig. 4. Th-232, K-40, and Ra-226 activity concentration.

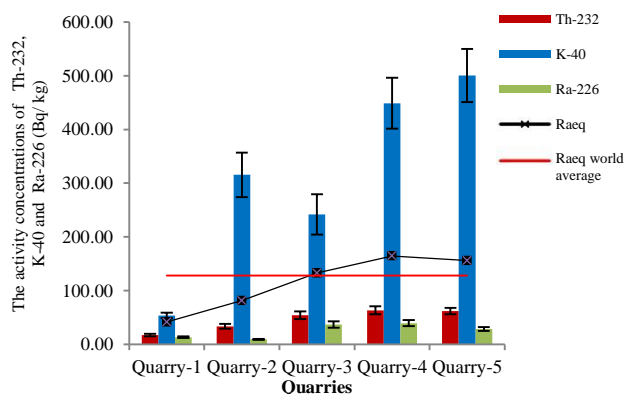


Fig. 5. Th-232, K-40, and Ra-226 activity concentration.

### Absorbed dose rate in air (D)

The population-weighted values give an absorbed dose rate in air outdoor from terrestrial gamma radiation a value of 59 nGy/h [18]. If adapted to exposure scenarios in this study, this gives a value of 0.29 mSv/year [ $59 \text{ nGy/h} \times 0.7 \text{ Sv/Gy} \times 8720 \times 0.8 \times 10^6$ ]. We take this value as a guide.

Figure 6 shows the largest value of the effective dose rate at site 9 (0.45 mSv/year), while the minimum value is recorded at site 5 (0.20 mSv/year). We can see values exceeding the limit for sites 1, 2, 3, 7, 8, and 9 (Fig. 6). However, in the case of site 9, this would be a natural marking given that this site is located outside the zones of influence of mining activities (Fig. 2). It would not be suitable for public use.

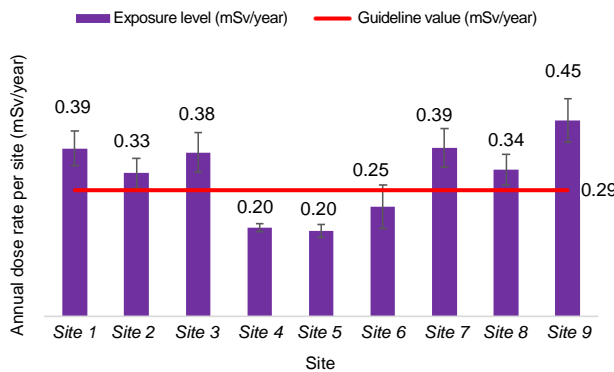


Fig. 6. Annual dose rate.

### Radiological hazard index

The results of the estimation of the radiological contamination indices of building materials (sand, gravel, and mud) are given in Table 1 below. The  $H_{ex}$ ,  $H_{in}$ , and  $I_y$  indices are all less than unity for all quarries except mud quarry and gravel (quarries 4 and 5), where  $I_y$  is found to be greater than one.

Thus, the two sand quarries and the gravel quarry (Quarry 3) do not present any hazard. On the other side, the gravel quarry (Quarry 4) as well as the mud quarry (Quarry 5) present risks of over exposure to ionizing radiation. The use of these two quarries would therefore be contraindicated for building purposes.

Table 1. Hazard indices of quarries samples.

Sample code	$H_{ex}$	$H_{in}$	$I_y$
Quarry-1	0.11	0.15	0.29
Quarry-2	0.22	0.25	0.61
Quarry-3	0.36	0.46	0.95
Quarry-4	0.44	0.55	1.20
Quarry-5	0.42	0.50	1.15

### Comparison of the results obtained in this study with the values reported in other countries worldwide

Tables 2 and 3 present the results obtained in this study and similar studies from different environments. The activity concentrations of Ra-226, Th-232, and K-40 obtained in this study is greater than the one obtained in Cameroon [7], United Kingdom [6], Hong Kong [27], and Nigeria [29]. In the case of the  $Ra_{eq}$  values, the result obtained in this study are higher than those of the other countries listed in Table 2, with the exception of Brazil [26] and Malaysia [28].

On the other hand, the D and  $H_{ex}$  values found in this study (Table 3) are lower than those obtained in Egypt [9], Pakistan [10], and Vietnam [35]. However, the  $I_y$  value found in our case is much higher than those found in Egypt [9] and Pakistan [10], the two countries listed in Table 3 for which this parameter was determined.

Table 2. Comparison of the Ra-226, Th-232, K-40 and  $Ra_{eq}$  values with the values reported in other countries worldwide.

Country	Ra-226	Th-232	K-40 (Bq/kg)	$Ra_{eq}$	References
Cameroon	27±4	15±1	277±16	70	[7]
Egypt	36.6±4.4	43.2±2.2	82±4.1	103	[21]
China	33.1	21.8	833.3	-	[22]
Zambia	23±2	32±3	134±13	79±11	[23]
India	37	24.1	432.2	104.7	[24]
Sweden	55	47	241	-	[20]
Italy	38±14	22±14	218±2	92±60	[25]
Pakistan	51	70	532	-	[36]
Brazil	61.7	58.5	564	188.8	[26]
United Kingdom	22	18	155	-	[6]
Hong Kong	19.2	18.9	127	-	[27]
Malaysia	51±1.0	23±1.0	823±69	188±27	[28]
Nigeria	2.16	7.82	114.3	19.7	[29]
Turkey	11.4	18.3	510.2	-	[30]
Bangladesh	57.5	25.4	255	-	[31]
Niger	29.41	49.27	380.61	129.18	Present Study
World average	32	45	412	129	UNSCEAR (2010) [20]

Table 3. Comparison of the D,  $H_{ex}$  and  $I_y$  values with the values reported in other countries worldwide.

Location	D(mSv/y)	$H_{ex}$	$I_y$	Reference
Egypt	145,16	0.4	0.52	[9]
India	0.12	-	-	[32]
Jordan	0.06	0.28	-	[33]
Malaysia	0.169	0.859	-	[4]
Pakistan	0.34	0.39	0.14	[10]
Saudi Arabia	0.14	0.13	-	[34]
Vietnam	0.54	0.43	-	[35]
Niger	0.32	0.31	0.84	Present Study

## CONCLUSION

The study concerned demonstration of the presence of natural radionuclides and the level of their original or enhanced activity concentration due to mining activities in the city of Arlit. The environmental matrices considered are essentially the soil and the building materials quarries used by the population (sand, gravel, and mud). Interpretation of the results of the analyzes show that six sites (1, 2, 3, 7, 8, and 9) exhibit a relatively high level of radioactivity. Indeed, the values (in nGy/h) are, respectively, 78.62, 67.06, 76.94, 78.98, 68.74, and 91.95, while the population-weighted values give an absorbed dose rate in air outdoor from terrestrial gamma radiation a value of 59 nGy/h. Likewise, the results showed that two (2) quarries are radiologically marked. These are the mud quarry ( $I_\gamma = 1.15$ ) and the gravel quarry ( $I_\gamma = 1.20$ ). In both cases,  $I_\gamma$  exceeds unity, which is the threshold value. However, the study does not attribute this marking exclusively to mining activities.

Indeed, for some sites, the anomaly observed could be linked to the geological nature of the area, as it is the case for site 9 which is far from the area of influence of the activities. On the other hand, the determination of the annual dose rate (D) and the hazards indices ( $H_{ex}$ ,  $H_{in}$  and  $I_\gamma$ ), are not required according to national radiation protection regulations. This study, therefore, encourages the reviewing and the updating of the existing legal framework in order to take into account the major concerns of overexposure to radioactivity of the populations.

## ACKNOWLEDGMENT

We especially thank Dr CISSE Djibrilla for the fruitful collaboration we have obtained with the National Office of Environmental Assessment of Niger (BNEE), in his capacity as Director General.

## AUTHOR CONTRIBUTION

All authors contributed to the study conception and design. The first draft of the manuscript was written by Oumarou Sidibe Mahamadou and all authors commented on previous versions of the manuscript. All authors read and approved the final manuscript.

## REFERENCES

1. R. Mehra, Indoor Built Environ. **18** (2009) 270.
2. M. A. Adam and M.A. Eltayeb, J. Environ. Radioact. **107** (2012) 23.
3. Lyngkhoi and P. Nongkynrih, Egypt. J. Basic Appl. Sci. **7** (2020) 194.
4. G. Alzubaidi, F. B. S. Hamid and I. A. Rahman, Sci. World J. **1** (2016) 1.
5. L. A. Najam and S. A. Younis, Int. J. Novel Res. Phys. Chem. Mathematics **2** (2015) 1.
6. J. Beretka and P. J. Mathew, Health Phys. **48** (1985) 87.
7. M. Ngachin, M. Garavaglia, C. Giovani *et al.*, Radiat. Meas. **42** (2007) 61.
8. Y. Kobya, H. Taskin H, C.M. Yeslkanat *et al.*, J. Radioanal Nucl. Chem. **303** (2015) 287.
9. S. U. EL-Kameesy, S. A. EL-Fiki, M. S. Talaat *et al.*, Global J. Phys. **4** (2016) 250.
10. M. Rafique, H. Rehman and M. Matiullah, Iran J. Radiat. Res. **9** (2011) 77.
11. A. Abdoul Aziz and J. Oumarou, *Environnement Géologique des Gisements d'Uranium dans les formations carbonifères de la bordure ouest du massif de l'air*, in: Report: INIS-NE--0002 (French), Inter. Nucl. Info. Syst. **39** (1968) 16.
12. M. Pagel, S. Cavellec, P. Forbes, *Uranium Deposits in the Arlit Area (Niger)*, in: Proceedings of the Springer-Verlag Berlin Heidelberg Conference **1** (2005) 303.
13. T. Sempere and B. Beaudoin, Bull. Soc. Géol. France **26** (1984) 995.
14. Food and Agriculture Organization (FAO), Harmonized World Soil Database, Rome (2009) 1.
15. Food and Agriculture Organization of The United Nations (FAO), L'irrigation en Afrique en chiffres Enquête AQUASTAT, Rome (2005) 1.
16. G. F. Knoll, Radiation Detection and Measurements, 3rd ed., John Wiley & Sons, Inc., New York (2000) 65.
17. Syarbaini, A. Warsona and D. Iskandar, Atom Indones. **40** (2014) 27.
18. United Nations Scientific Committee on the Effects of Atomic Radiation (UNSCEAR), *Sources and Effects of Ionizing Radiation*, in: Report to the General Assembly, with Scientific Annexes, New York (2000) 1.

19. United Nations Scientific Committee on the Effects of Atomic Radiation (UNSCEAR), *Sources and Effects of Ionizing Radiation*, in: Report to the General Assembly, with Scientific Annexes, New York (1993) 1.
20. Nuclear Energy Agency (NEA) - Organisation for Economic Cooperation and Development (OECD), *Exposure to Radiation from the Natural Radioactivity in Building Material*, in: Report by a Group of Experts, Paris (1979) 1.
21. El-Taher, Radiat. Prot. Dosim. **138** (2010) 166.
22. X. Lu, X. Zhang and F. Wang, Environ. Earth Sci. **53** (2007) 1475.
23. P. Hayumbu, M. B. Zaman, N. C. H. Luhaba *et al.*, J. Radioanal. Nucl. Chem. **199** (1995) 229.
24. V. Kumar, T. V. Ramachandran and R. Prasad, Appl. Radiat. Isot. **51** (1999) 93.
25. S. Rizzo, M. Brai, S. Basile *et al.*, Appl. Radiat. Isot. **55** (2001) 259.
26. Malanca, V. Pessina, G. Dallara *et al.*, Appl. Radiat. Isot. **46** (1995) 1387.
27. K. N. Yu, Z. J. Guan, M. J. Stokes *et al.*, J. Environ. Radioact. **17** (1992) 31.
28. N. Ibrahim. J. Environ. Radioact. **43** (1999) 255.
29. K. Ademola, O. P. Ademola, M. A. Fatai *et al.*, Nucl. Radiat. Phys. **102** (2017) 44416.
30. H. Eroglu and O. Kabadayi, Radiat. Prot. Dosim. **156** (2013) 331.
31. M. I. Chowdhury, M. N. Alam and S. K. S. Hazari, Appl. Radiat. Isot. **51** (1999) 747.
32. R. Mehra and M. Singh, J. Environ. Prot. **2** (2011) 960.
33. F. Al-Hamarneh and M. I. Awadallah, Radiat. Meas. **44** (2009) 102.
34. S. Alaamer, Turkish J. Eng. Environ. Sci. **32** (2008) 229.
35. N. Q. Huy, P. D. Hien, T. V. Luyen *et al.*, Radiat. Prot. Dosim. **151** (2012) 522.
36. A. A. Qureshi, S. Tariq, K. U. Din *et al.*, J. Radiat. Res. Appl. Sci. **7** (2014) 438.